JCTC Journal of Chemical Theory and Computation

ARTICLE

pubs.acs.org/JCTC

Silicon Nanocrystal Functionalization: Analytic Fitting of DFTB Parameters

Fabio Trani*[,†,‡] and Vincenzo Barone[†,‡]

[†]Scuola Normale Superiore, Piazza dei Cavalieri 7, 56126, Pisa, Italy

[‡]Infn Sezione di Pisa

ABSTRACT: A density functional tight binding (DFTB) scheme has been applied to functionalized silicon nanocrystals. Using an analytic functional representation of DFTB parameters, the scheme has been used to compute the adsorption energies in the organic functionalization of reconstructed Si(100) and H-terminated Si(111) surfaces of hundreds-of-atoms nanocrystals. We adopt an ONIOM(QM:QM′) approach that corrects the overbinding of DFTB, obtaining nice agreement with high-level reaction energies and structural configurations.

1. INTRODUCTION

The synthesis of bright, stable, water-soluble silicon nanocrystals has opened the route to realistic biomedical applications of functionalized silicon nanoparticles as cellular probes.[1−3] The recent chemical synthesis techniques allow for an excellent control of nanoparticle size-dispersion, shape, and passivation that allows a suitable design of their fluorescence properties.[1] As is well-known, the chemical environment plays the role of a key agent that can deeply modify the nanocrystal electronic structure and optical spectra. Oxygen-free silicon nanostructures, for instance, alkyl-terminated nanocrystals, are characterized by a strong photoluminescence, with high quantum yield, in the blue spectral region.[4] This new generation of blue-emitting, water stable silicon nanocrystals makes them ideal candidates for applications in medical biosensing, in particular as fluorescent tumoral markers.[3,5,6] At variance with other compounds, such as CdSe nanorods, silicon nanocrystals are nontoxic and biocompatible, and this justifies the enormous interest in such materials.

On the theoretical side, several papers have been published on the functionalization of silicon nanocrystals,[7−9] but comprehensive studies are still lacking. New integrated computational approaches are currently being developed to simulate the interaction of silicon nanocrystals with biological systems. In particular, many body and density functional approaches allow for the description of few-nanometer structures, while huge, realistic nanocrystals, functionalized by large organic molecules (such as DNA fragments or organic dyes), have hardly been studied because of the demanding resources required. A detailed description of the mutual interplay between the silicon nanoparticle excited states and the energy levels of biological molecules can lead to very promising results, with high impact technological implications.

Density functional tight binding is a powerful approach that has been receiving wide interest from the computational chemistry community, because of its reliable description of organic molecules, as well as that of inorganic structures.[10−15] The method gives an accurate description of the core Hamiltonian, better than the standard quantum chemistry semiempirical approaches. Furthermore, it takes into account the charge transfer in a self-consistent way (self-consistent charge density functional tight binding), thus allowing for an accurate prediction of covalent and ionic bonds. [The self-consistent charge density functional tight binding is usually named SCC-DFTB. For the sake of simplicity, we use in the whole paper the notation DFTB for the SCC-DFTB approach.] The method has been used for the description of organic molecules as a high level approach in a QM/MM multilevel scheme,[12] or as a low-level method in QM/QM′.[16] A recent extension of the method to include third-order expansion of the total energy has been shown to improve the description of hydrogen-bonding interactions and proton affinities of biological systems.[17] Moreover, the time dependent extension of the method (TD-DFTB) is becoming a very powerful and reliable tool to calculate the spectroscopic properties of biological systems and nanomaterials.[18,19] Another important field of application is in solvation effects and simulations of molecules in solution.[20]

In all of these issues, the calculation of the forces is very challenging, and the availability of explicit, analytic gradients is in most cases an invaluable tool in speeding up the procedure. This motivated us to do an analytic fitting of DFTB parameters for applications to nanomaterials.

In this paper, an analytic formulation of DFTB parameters for silicon-based materials is provided. The first part of the paper is devoted to the description of the fitting procedure of a tabulated set of DFTB parameters involving silicon, with a presentation of the results of the fitting. In the second part, the method is applied to the description of functionalized silicon nanocrystals and is checked against more accurate results. Among the many possible applications, we show how DFTB can be used together with density functional theory in a multilevel approach, based on an ONIOM scheme,[21,22] for a high-level description of hundreds-of-atoms functionalized silicon nanocrystals. It will be shown that the results obtained using ONIOM are very accurate, both in terms of the geometry and in terms of the energetics.

Received: October 25, 2010
Published: January 10, 2011

2. THE METHOD

Semiempirical tight binding approaches have been used for several years in the field of materials science.[23] The transferability of the parameters from the bulk to nanostructures made it a simple and transparent framework for describing the electronic properties of hundreds- to thousands-of-atoms systems.[24,25] However, the lack of reliable interaction parameters to represent the organic molecules was the main drawback of this approach, which was unfit to model hybrid organic−inorganic structures. With the progress of synthesis techniques and the use of nanostructures in realistic biotechnological applications, the theoretical problem has moved from the description of free-standing semiconductor nanocrystals to their interaction with an external organic environment, and the use of different, more reliable computational tools was required.

Quantum chemistry semiempirical approaches, such as MNDO, AM1, and PM6,[26] offer an invaluable tool for structural optimizations and reaction path descriptions of thousands-of-atoms structures. More accurate than classical force field models in all situations involving the breaking and formation of chemical bonds, semiempirical methods are very useful in characterizing organic molecules and small clusters. But the parametrization of the core Hamiltonian is often oversimplified. At variance with semiempirical approaches, DFTB furnishes a more complex parametrization of the core Hamiltonian that can lead to a more accurate treatment of the excited states, especially in complex environments like semiconductor nanocrystals.

DFTB is a method derived by a second-order expansion of the exact DFT Hamiltonian with respect to the electronic charge density variations.[27] The method is based on a minimal parametrization of the core Hamiltonian, where the onsite parameters (onsite energies, Hubbard terms, spin−spin interaction terms) are calculated from isolated atoms.[28] For the two center parameters, contracted Slater-type atomic orbitals are obtained from the solution of the Kohn−Sham equation for free atoms, where a confining potential is added to mimic the presence of a molecular or solid state environment. From the Slater-type atomic orbitals, the overlap integrals are calculated as a function of the atom−atom distance. Instead, the contracted atomic densities are used to form the interatomic potential of a diatomic molecule,[29] whose matrix elements with the contracted orbitals give the two-center interaction terms of the core Hamiltonian.[30] Repulsive interatomic energy E_{rep} takes into account the exchange-correlation contributions that are not included in the core Hamiltonian, in the self-consistent charge contribution, or in the spin−spin interaction terms.[15] It is written as a sum of two-body potentials V^{rep} and is obtained by comparison to DFT total energies. The parametrization of the repulsive term is a delicate point of the scheme. In particular, it strongly depends on the exchange-correlation functional chosen as a reference (GGA, B3LYP...) and determines the goodness of a DFTB parametrization. Automatic fitting schemes have been proposed in the literature, with the hope of providing a unique potential able to describe most of the features of interest (vibrational spectra, geometries, reaction path energetics, proton affinities).[31]

The method is competitive against semiempirical models for biological systems, where it has been used with a remarkable success.[16,28,32] For semiconductor nanocrystals, DFTB keeps the advantages of semiempirical tight binding for huge structures. It has been applied for time dependent calculations of excited state properties of silicon nanocrystals.[33,34] Recent efforts propose

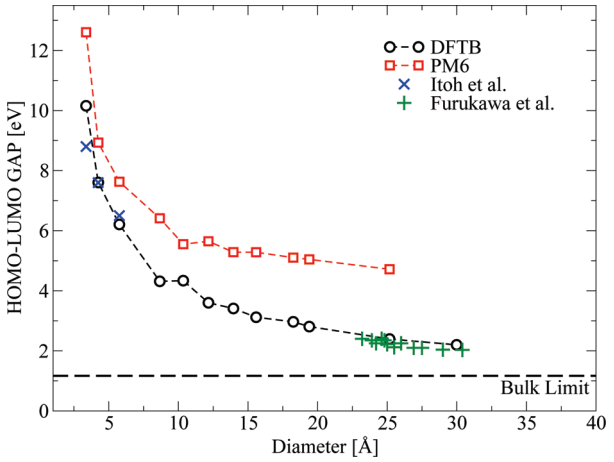

Figure 1. The energy gap of silicon nanocrystals as a function of their size. DFTB and PM6 results are respectively indicated in black circles and red squares. Experimental data for small-[37] and medium-size[38] nanocrystals are shown as blue crosses and green plus symbols. The lines are guides for the eyes.

DFTB parametrizations that can be applied as well to periodic systems, showing that the method is able to fairly reproduce the band structures.[35,36] Thus, if well parametrized, the method is virtually able to cover a wide range of systems, from molecular systems to thousands-of-atoms structures, from nanowires to slabs to bulk systems. But, as a matter of fact, the quality of the results depends on the parametrization.

A common benchmark used to check the validity of a parametrization to describe semiconductor nanostructures is the prediction of the optical gap as a function of the size.[24] In Figure 1, the highest occupied molecular orbital (HOMO) to lowest unoccupied molecular orbital (LUMO) energy gap is reported for a set of silicon nanocrystals, upon increasing their size. The energy gap was calculated using DFTB and PM6. As a comparison, experimental data of optical gaps for small- and medium-size nanocrystals are shown, together with the indirect gap of bulk silicon. The calculations have been done using the Gaussian package,[39] with the *pbc-0-3* set of parameters for DFTB.[40] The nanocrystals were built cutting silicon clusters of spherical shape, with a silicon atom in the center, and terminating all the surface atoms with hydrogen.[25] To have an idea of the number of atoms, $Si_{705}H_{300}$ is the largest nanocrystal here considered (3 nm diameter), while $Si_{191}H_{148}$ corresponds to a 2 nm diameter nanocrystal. Figure 1 shows that this set of parameters nicely reproduces the gap energies for silicon nanocrystals. The DFTB results cross the experimental data, and they tend to the correct limit of the indirect band gap of bulk silicon. It is known that for small molecules the correlation effects can be significant, and the experimental gap, measured from the absorption threshold or photoluminescence spectra, usually differs from the HOMO−LUMO gap. But such a difference becomes negligible upon increasing the size, and for huge nanocrystals, the HOMO−LUMO gap represents quite an accurate estimation of the absorption threshold. The main result is that DFTB reproduces the right trend of the energy gap versus the size. On the contrary, the accuracy of PM6 is significantly reduced upon increasing the nanocrystal size, and for hundreds-of-atoms structures, the results are several electronvolts far from the bulk limit.

It is known from the literature that a minimal basis set can hardly reproduce the bulk silicon conduction bands, and either

an extended basis set[41] or a three-center parametrization[24] is needed for an accurate reproduction of the band structures. Figure 1 demonstrates that, while PM6 is unable to reproduce the electronic spectra, going to a large energy gap for huge nanocrystals, DFTB can be used for UV/vis spectra calculations, since it yields the correct trend of the energy gap with the size. Nevertheless, a quantitative treatment of the excited states can be performed only after an improvement of the DFTB parametrization, which has to furnish accurate band structures for the bulk limit, as has been recently shown with TiO_2 and ZnO parametrizations.[35,36] Work along these lines is in progress.

3. DFTB ANALYTIC PARAMETRIZATION

A version of the DFTB method was recently implemented in the Gaussian package,[39] based on the analytic fitting of the Hamiltonian and overlap matrix elements, as well as that of the interatomic repulsive term.[13,15] The great advantage of using an analytic formulation of DFTB parameters consists in having a functional form for the energy gradients and Hessians, which do not need to be calculated numerically.[32,42,43] Starting from an existing parametrization, we performed an analytic fitting of the tabulated DFTB parameters (Hamiltonian, overlap, and repulsive potential) adopting a functional representation implemented in Gaussian.

We used the *pbc-0-3* set of parameters.[40] The Si−Si parameters were initially developed by Frauenheim et al.[44] They were later modified by Sieck to include a self-consistent charge contribution.[30] As we show in Figure 1, this parametrization describes free-standing silicon nanocrystals well. But the method only gives qualitative results for organic molecules. We thus integrate the parameters of Si−Si and Si−X interactions, to the set already present in Gaussian,[39] which is more accurate in describing biological systems.[16] In the original DFTB set of parameters, the overlap and Hamiltonian matrix elements are tabulated for a dense mesh of interatomic distances. Instead, the repulsive potential is represented using a collection of cubic splines. Cubic splines are not a good approach for the calculation of Hessians, because of piecewise linear functions in the second-order derivatives. For this reason, automatic procedures to calculate the repulsive potentials were recently proposed, with the use of higher-order splines, to get sufficiently smooth functions to adequately reproduce the Hessian.[31] The use of an analytic functional form overcomes this problem, with smooth second-order derivatives.

We used the following functional form, implemented in Gaussian, for the fitting:

$$F(R) = \sum_{i=1}^{10} C_i \exp(-\alpha\beta^i R) \qquad (1)$$

The fitting scheme was based on a trust region algorithm to obtain a starting estimation of the solution, followed by a Levenberg−Marquard algorithm to reach high precision results. The procedure was repeated starting from several initial configurations, in order to minimize the dependence on the starting guess. As an example of the accuracy of our results, we report in Figure 2 the overlap and Hamiltonian Si−Si sp matrix elements, and the repulsive potential, according to the tabulated set of parameters, and calculated using the fitted values. We also report in the insets the error, defined as the difference between the curves. The redundant functional form reported in eq 1 produces artificial oscillations at large interatomic separation. As much as we could, we reduced the oscillating behavior near the cutoff radius (see Figure 2), but the oscillations cannot be fully deleted. A major problem related to them is the presence of a discontinuity at the cutoff radius that leads to divergences in the calculation of energy gradients. In order to solve this problem, beyond a given value (chosen at $0.85R_{cutoff}$), in the Gaussian package,[39] the analytic expression in eq 1 is multiplied by a polynomial function that makes the curve smoothly tend toward zero.

In Table 1, the root-mean-square errors are reported for the Si−X (X = Si, C, H, O, N) DFTB parameters. It can be observed that the fitting scheme works better for overlap and Hamiltonian matrix elements, while for the repulsive potential, the errors are slightly larger, albeit still satisfactory. We checked the analytic parameters against the tabulated ones for several molecules and found accurate geometries and total energies. We underline that the use of a functional form for the parameters does not modify the quality of the results, which are uniquely determined by the tabulated parametrization described in the literature.[30]

4. RESULTS

In this section, a few applications of the method for functionalized silicon nanocrystals are reported. First, we studied the adsorption of organic molecules on the Si(100) surface of silicon nanocrystals with increasing size. We take as a case study the 1-amino-3-cyclopentene (ACP) adsorption, which is a significant example of [2 + 2] cycloaddition of a cyclic organic molecule with an amino group, on the Si(100) reconstructed surface.[45] The results have been much debated in the literature, especially in regard to their unexpected difference, even within density functional theory, upon changing the basis set, the exchange-correlation functional, the model used to simulate the system. Non-negligible variations of the energetics were reported when moving from pseudopotential to all-electron basis sets, from GGA to B3LYP functionals, and from cluster to periodic surface models.[45,46] Nevertheless, the PBE0 exchange-correlation functional has been shown to give reaction path energetics comparable to MP2 results.[46] We thus performed DFT calculations using Gaussian,[39] with the PBE0 functional and the recently developed N07D basis set.[47]

We first considered the ACP adsorption on the small nanocrystals previously studied in the literature, Si_9H_{12} and $Si_{29}H_{32}$;[45] then we increased the nanocrystal size. But, instead of simply choosing a spherical shape, with lots of single-bonded silicon atoms at the surface, we chose a more compact shape and a smaller number of H terminations. The nanocrystals are fully H-passivated except for a Si−Si dimer on the (100) surface. In Figure 3, the ACP-functionalized silicon nanocrystals are shown for several sizes.

For small nanocrystals, we performed PBE0/N07D calculations, and a direct comparison with DFTB calculations was possible. The results are reported in Table 2. We found that, while DFTB correctly reproduces the geometry, the adsorption energies are more than 10 kcal mol^{-1} too large in absolute value. The tendency of DFTB to overbind is known in the literature, as well as its accuracy in reproducing molecular structures.[48,49] In the present case, the systematic error could be due to the pure exchange-correlation functional used as a reference in the parametrization. In order to determine the origin of the overbinding, we performed local spin-density calculations (LSDA) for small nanocrystals, using the N07D basis set, and report the results in

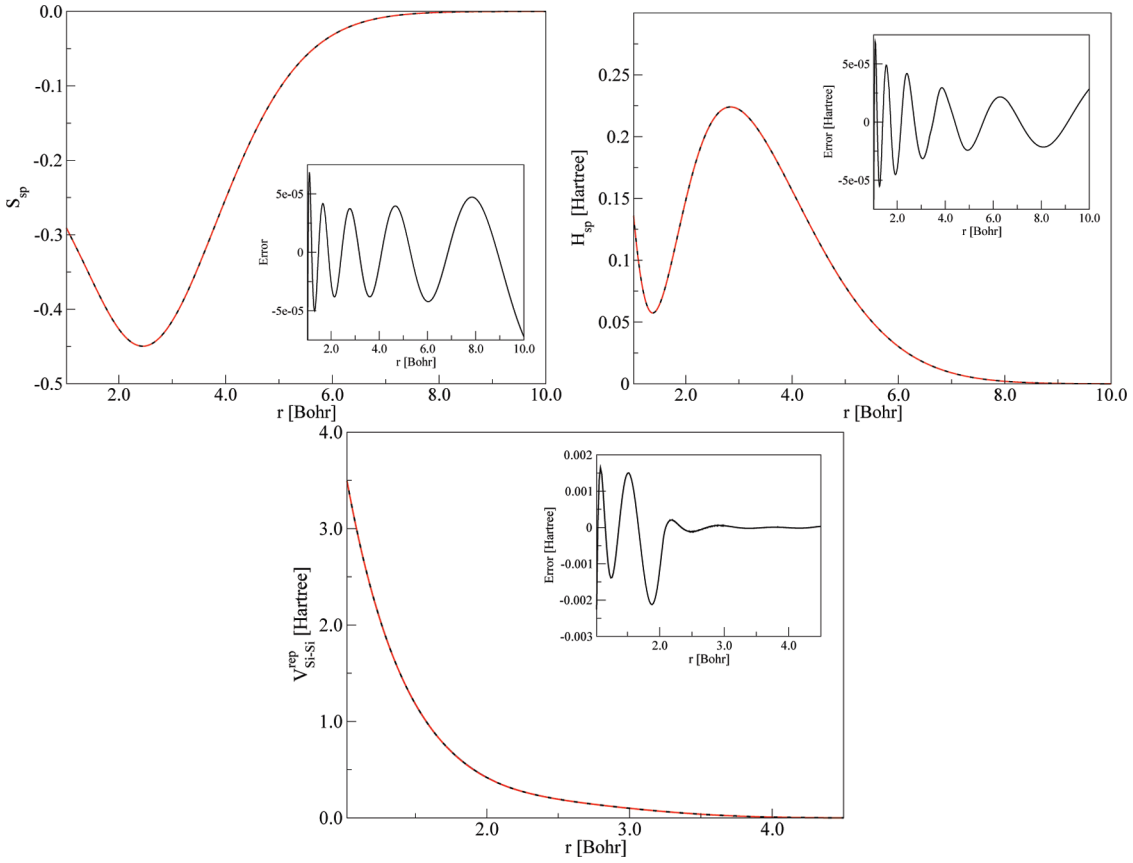

Figure 2. Some results obtained applying the fitting scheme to Si−Si parameters. The overlap and Hamiltonian matrix elements for the sp interaction, and the repulsive potential, are shown as a function of the interatomic distance. Black solid lines refer to the *pbc-0-3* tabulated parameters.[30,44] Red dashed lines are the curves obtained as a result of the fitting. The errors, defined as difference between reference data and fitted values, are reported in the insets.

Table 1. Root Mean Square of the Difference between the Analytic Fitting and the Original Set of Parameters, for Overlap, Hamiltonian Matrix and Repulsive Potential (Energies in Hartree)

	Si−Si	Si−C	Si−H	Si−O	Si−N
S	2.0×10^{-5}	9.0×10^{-6}	5.1×10^{-6}	3.1×10^{-6}	3.2×10^{-6}
H^0	2.1×10^{-5}	1.0×10^{-5}	8.9×10^{-6}	9.5×10^{-6}	4.3×10^{-6}
V^{rep}	1.4×10^{-4}	5.6×10^{-4}	6.8×10^{-5}	1.3×10^{-4}	1.6×10^{-4}

the last column of Table 2. There is nice agreement with DFTB; the adsorption energies correspond within 2 kcal mol^{-1}. Thus, the DFTB error could have been inherited by the well-known LDA overbinding.[46,50]

An interesting improvement consists in performing ONIOM-(QM:QM′) calculations, with DFTB as a low-level approach and density functional theory as a high-level method, as recently proposed for the study of enzymes.[16] Previous ONIOM calculations have shown that it can be a powerful approach to the description of functionalized silicon surfaces.[51] We used DFT PBE0/N07D for high-level calculations on the model system and DFTB in its analytic formulation for calculations on the real system. According to the ONIOM scheme, the DFT total energy of a huge functionalized silicon nanocrystal is estimated as

$$\Delta E^{\mathrm{ONIOM}} = \Delta E^{\mathrm{DFTB}}(R) + \Delta E^{\mathrm{DFT}}(M) - \Delta E^{\mathrm{DFTB}}(M) \quad (2)$$

In the previous equation, R is the real system (ACP on the whole nanocrystal), while M is the model system, constituted by ACP and the nanocrystal active site.

A delicate point in using ONIOM approaches consists in the choice of the model system. In the present work, it is constituted by the organic molecule, ACP, and the smallest cluster here considered, Si_9H_{12}. In Figure 4, we graphically report the ONIOM scheme for ACP on $Si_{158}H_{96}$. The part used for the model system is highlighted; the remaining part of the nanocrystal is only calculated within DFTB. We report in Table 2 the results obtained for several nanocrystals. It can be noted that the ONIOM approach represents a large improvement over DFTB. For both the nanocrystals that we used for the comparison, $Si_{29}H_{32}$ and $Si_{33}H_{32}$, the relative error in the energetics decreases from about 21−24% to 1−2%, with an absolute error smaller than 1 kcal mol^{-1}. In particular, the ONIOM approach works better for the more compact nanocrystal $Si_{33}H_{32}$. It is interesting that, while DFTB adsorption energies are almost independent of the size (small to big) and the shape (decrease of H terminations), the ONIOM approach allows for the recovery of a dependence on the size and shape that is in good agreement with PBE0. Moreover, as expected, the adsorption energy changes very little for the largest nanocrystals. The adsorption energy limit has a value that is in fair agreement with PBE0 results.

In Table 3, the main structural data are reported for the optimized configurations of ACP on $Si_{29}H_{32}$. The geometries have been obtained using DFTB, PBE0/N07D, and the ONIOM

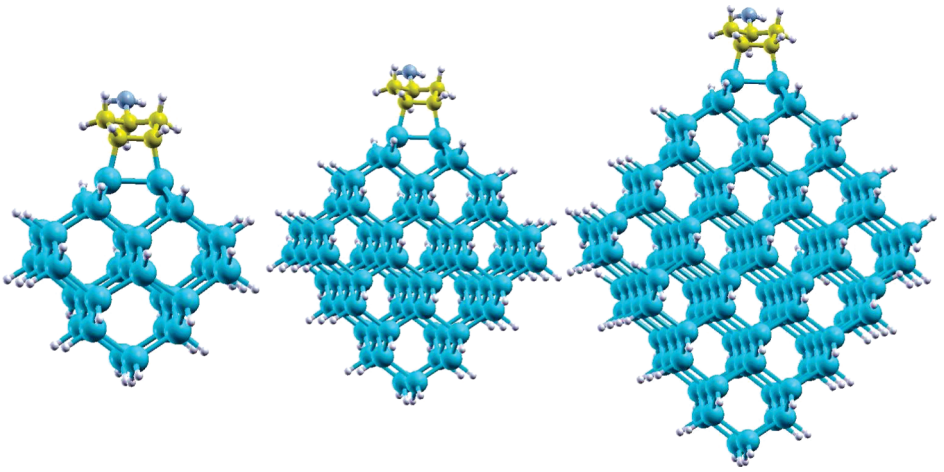

Figure 3. ACP adsorption on $Si_{33}H_{32}$, $Si_{82}H_{60}$, and $Si_{158}H_{96}$.

Table 2. Adsorption Energies for a [2 + 2] Cycloaddition Reaction of ACP on the Si(100) Surface, for Several Nanocrystals of Increasing Size [Energies in kcal mol^{-1}]

	DFTB	ONIOM	PBE0	LSDA
Si_9H_{12}	−60.99		−47.29	−59.51
$Si_{29}H_{32}$	−60.45	−47.80	−48.88	−61.12
$Si_{33}H_{32}$	−60.52	−49.33	−49.98	−62.22
$Si_{82}H_{60}$	−60.51	−50.06		
$Si_{158}H_{96}$	−60.46	−50.13		

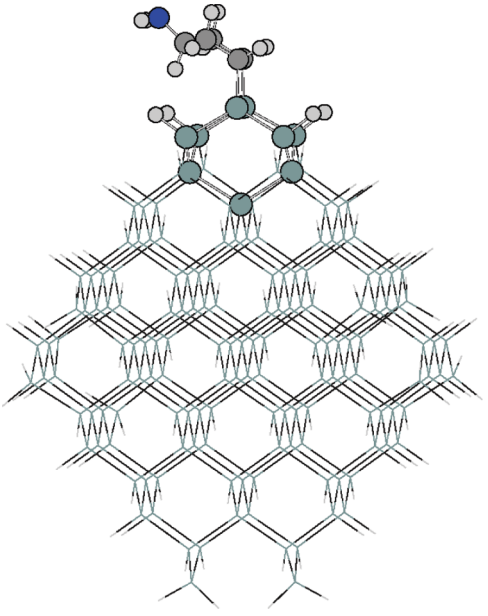

Figure 4. ACP functionalization of $Si_{158}H_{96}$. The part highlighted in the picture constitutes the model system used for ONIOM calculations.

approach previously described. In agreement with the literature, we find that DFTB is a valid tool to perform fast structural optimizations, with a fair agreement with a high-level approach. Indeed, the errors are smaller that 0.02 Å for the lengths, and 1° on the angles, with respect to the PBE0 calculation. The slight underestimation of the Si−C distances is an artifact of the DFTB

Table 3. Optimized Geometry for the Adsorption of an ACP Molecule on $Si_{29}H_{32}$[a]

	DFTB	ONIOM	PBE0
Si(1)−Si(2)	2.348	2.348	2.345
Si(2)−Si(3)	2.344	2.362	2.358
Si(1)−C(1)	1.947	1.956	1.959
C(1)−C(2)	1.56	1.583	1.582
Si(3)−Si(2)−Si(4)	111.6	110.6	111.1
Si(1)−C(1)−C(2)	101.7	101.3	101.2

[a] The lengths are in Å, the angles in degrees. Labeling of atoms follows Festa et al.[45]

overbinding, and it could be overcome by an improved parametrization. Using the ONIOM approach as described above, the errors decrease dramatically, becoming smaller than 0.004 Å for the distances.

To conclude, it is worth noting that, using just a few silicon atoms for the model system, the ONIOM approach yields results comparable to full DFT/PBE0 calculations, proving geometries and energies for hundreds-of-atoms nanocrystals, with a much lighter computational effort.

As a second case, we studied the adsorption of an allylamine molecule on the Si(111) surface, whose interest for DNA sensing is huge.[52,53] In particular, the functionalization with a propylamine chain was studied upon increasing the H-terminated Si(111) surface area and depth. At variance with the first case (ACP on silicon nanocrystals), the clusters have been modeled to be almost conically shaped, in order to represent a piece of a surface. Just like before, we studied the smallest cluster, Si_4H_{10}, then $Si_{16}H_{28}$, and, finally, a hundreds-of-atoms cluster, $Si_{109}H_{88}$. The results are reported in Table 4.

Also in this system, there is an overbinding of DFTB with respect to PBE0/N07D, with a large relative error. We performed LSDA calculations, to see whether in this case there is agreement with DFTB, too. As reported in Table 4, the trend is confirmed, but in this case, DFTB results show a larger overbinding than LSDA. In order to understand the role of the different interaction terms in DFTB, we performed some calculations on small systems, from which it emerges that the main source of error could rely on the parametrization of the Si−C repulsive term.

Table 4. Reaction Energies for the Functionalization of a Si(111) Surface by Propylamine [Energies in kcal mol^{-1}]

	DFTB	ONIOM	PBE0	LSDA
Si_4H_{10}	−54.48		−32.95	−43.47
$Si_{16}H_{28}$	−54.47	−32.88	−32.29	−47.61
$Si_{109}H_{88}$	−54.78	−33.54		

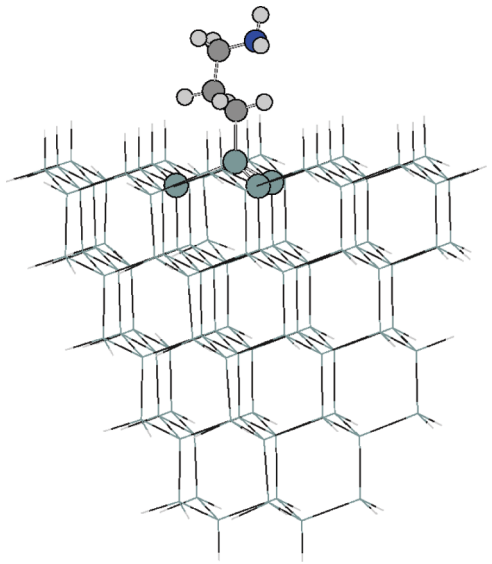

Figure 5. Functionalization of $Si_{109}H_{88}$ with a propylamine chain. Illustration of the model system in ONIOM.

Just like before, we applied an ONIOM(DFT:DFTB) approach, where both the chain and the minimal cluster (Si_4H_{10}) form the model system. Figure 5 illustrates the use of ONIOM in this situation, and the conical shape that we used to model the surface. In this case, the number of atoms in the model system is so small that the ONIOM calculations are extremely fast. Even in this system, the ONIOM approach largely corrects the DFTB overbinding, with an absolute error smaller than 1 kcal mol^{-1}.

5. CONCLUSIONS

An analytic parametrization of DFTB has been proposed for Si-based materials, on the grounds of the DFTB method implemented in the Gaussian computational suite. The method allows the description of thousands-of-atoms structures, in particular, the organic functionalization of silicon surfaces and nanocrystals. As an illustration of the method, we applied the method to the adsorption of ACP on the (100) surface of Si nanocrystals, and the propylamine functionalization of Si(111) surfaces. We found an overbinding in the energetics of about 10 kcal mol^{-1} and more than 20 kcal mol^{-1}, respectively. Nevertheless, using an ONIOM(DFT:DFTB) approach with only a few atoms close to the nanocrystal active site, good agreement with DFT/PBE0 results is gained, with a drastic decrease of the relative error, and an accuracy better than 1 kcal mol^{-1} on the adsorption energies. Work along an improvement of the parametrization, and the use of the ONIOM approach for the study of huge functionalized silicon nanostructures, is in progress.

AUTHOR INFORMATION

Corresponding Author
*E-mail: fabio.trani@sns.it.

ACKNOWLEDGMENT

The authors thank Giacomo Prampolini, for support on the fitting scheme. Part of the calculations have been performed using the CASPUR advanced computing facilities.

REFERENCES

(1) Warner, J.-H.; Hoshino, A.; Yamamoto, K.; Tilley, R. D. *Angew. Chem., Int. Ed.* **2005**, *44*, 4550–4554.
(2) He, Y.; Kang, Z.-H.; Li, Q.-S.; Tsang, C. H. A.; Fan, C.-H.; Lee, S.-T. *Angew. Chem., Int. Ed.* **2009**, *48*, 128.
(3) Erogbogbo, F.; Yong, K.-T.; Roy, I.; Xu, G.; Prasad, P. N.; Swihart, M. T. *ACS Nano* **2008**, *2*, 873–878.
(4) Rosso-Vasic, M.; Spruijt, E.; van Lagen, B.; De Cola, L.; Zuilhof, H. *Small* **2008**, *4*, 1835–1841.
(5) Lin, V. S.-Y. *Nat. Mater.* **2009**, *8*, 252–253.
(6) Park, J.-H.; Gu, L.; von Maltzahn, G.; Ruoslahti, E.; Bhatia, S. N.; Sailor, M. J. *Nat. Mater.* **2009**, *8*, 331–336.
(7) Reboredo, F. A.; Galli, G. *J. Phys. Chem. B* **2005**, *109*, 1072–1078.
(8) Puzder, A.; Williamson, A. J.; Grossman, J. C.; Galli, G. *Phys. Rev. Lett.* **2002**, *88*, 097401.
(9) Li, Q. S.; Zhang, R. Q.; Lee, S. T.; Niehaus, T. A.; Frauenheim, T. *J. Chem. Phys.* **2008**, *128*, 244714.
(10) Frauenheim, T.; Seifert, G.; Elstner, M.; Niehaus, T.; Kohler, C.; Amkreutz, M.; Sternberg, M.; Hajnal, Z.; Di Carlo, A.; Suhai, S. *J. Phys.: Condens. Matter* **2002**, *14*, 3015.
(11) Aradi, B.; Hourahine, B.; Frauenheim, T. *J. Phys. Chem. A* **2007**, *111*, 5678–5684.
(12) de M. Seabra, G.; Walker, R. C.; Elstner, M.; Case, D. A.; Roitberg, A. E. *J. Phys. Chem. A* **2007**, *111*, 5655–5664.
(13) Zheng, G.; Witek, H. A.; Bobadova-Parvanova, P.; Irle, S.; Musaev, D. G.; Prabhakar, R.; Morokuma, K.; Lundberg, M.; Elstner, M.; Köhler, C.; Frauenheim, T. *J. Chem. Theory Comput.* **2007**, *3*, 1349–1367.
(14) de M. Seabra, G.; Walker, R. C.; Roitberg, A. E. *J. Phys. Chem. A* **2009**, *113*, 11938–11948.
(15) Zheng, G.; Lundberg, M.; Jakowski, J.; Vreven, T.; Frisch, M. J.; Morokuma, K. *Int. J. Quantum Chem.* **2009**, *109*, 1841–1854.
(16) Lundberg, M.; Sasakura, Y.; Zheng, G.; Morokuma, K. *J. Chem. Theory Comput.* **2010**, *6*, 1413–1427.
(17) Yang, Y. H.; York, D.; Cui, Q.; Elstner, M. *J. Phys. Chem. A* **2007**, *111*, 10861–10873.
(18) Niehaus, T. A.; Suhai, S.; Della Sala, F.; Lugli, P.; Elstner, M.; Seifert, G.; Frauenheim, T. *Phys. Rev. B* **2001**, *63*, 085108.
(19) Cui, G.; Fang, W.; Yang, W. *Phys. Chem. Chem. Phys.* **2010**, *12*, 416–421.
(20) Hou, G.; Zhu, X.; Cui, Q. *J. Chem. Theory Comput.* **2010**, *6*, 2303–2314.
(21) Dapprich, S.; Komaromi, I.; Byun, K.; Morokuma, K.; Frisch, M. *THEOCHEM* **1999**, *461−462*, 1–21.
(22) Vreven, T.; Byun, K. S.; Komaromi, I.; Dapprich, S.; Montgomery, J. A.; Morokuma, K.; Frisch, M. J. *J. Chem. Theory Comput.* **2006**, *2*, 815–826.
(23) Delerue, C.; Lannoo, M. *Nanostructures, Theory and Modelling; NanoScience and Technology*; Springer: Berlin, 2004; pp 31−38; 60−70; 112−128; 197−200.
(24) Niquet, Y. M.; Delerue, C.; Allan, G.; Lannoo, M. *Phys. Rev. B* **2000**, *62*, 5109–5116.
(25) Trani, F.; Cantele, G.; Ninno, D.; Iadonisi, G. *Phys. Rev. B* **2005**, *72*, 075423.
(26) Stewart, J. *J. Mol. Model.* **2007**, *13*, 1173–1213.

(27) Elstner, M.; Porezag, D.; Jungnickel, G.; Elsner, J.; Haugk, M.; Frauenheim, T.; Suhai, S.; Seifert, G. *Phys. Rev. B* **1998**, *58*, 7260–7268.
(28) Zheng, G.; Irle, S.; Morokuma, K. *Chem. Phys. Lett.* **2005**, *412*, 210–216.
(29) Porezag, D.; Frauenheim, T.; Köhler, T.; Seifert, G.; Kaschner, R. *Phys. Rev. B* **1995**, *51*, 12947–12957.
(30) Sieck, A. Ph.D. thesis, University of Paderborn, 2000. http://ubdata.uni-paderborn.de/ediss/06/2000/sieck (accessed Dec 06, 2010), pp 26−30;109−120.
(31) Gaus, M.; Chou, C.-P.; Witek, H.; Elstner, M. *J. Phys. Chem. A* **2009**, *113*, 11866–11881.
(32) Witek, H. A.; Irle, S.; Morokuma, K. *J. Chem. Phys.* **2004**, *121*, 5163.
(33) Li, Q. S.; Zhang, R. Q.; Lee, S. T.; Niehaus, T. A.; Frauenheim, T. *Appl. Phys. Lett.* **2008**, *92*, 053107.
(34) Wang, Y.; Zhang, R.; Frauenheim, T.; Niehaus, T. A. *J. Phys. Chem. C* **2009**, *113*, 12935.
(35) Moreira, N.; Dolgonos, G.; Aradi, B.; da Rosa, A.; Frauenheim, T. *J. Chem. Theory Comput.* **2009**, *5*, 605–614.
(36) Dolgonos, G.; Aradi, B.; Moreira, N. H.; Frauenheim, T. *J. Chem. Theory. Comput.* **2010**, *6*, 266–278.
(37) Itoh, U.; Toyoshima, Y.; Onuki, H.; Washida, N.; Ibuki, T. *J. Chem. Phys.* **1986**, *85*, 4867–4872.
(38) Furukawa, S.; Miyasato, T. *Phys. Rev. B* **1988**, *38*, 5726–5729.
(39) Frisch, M. J.; Trucks, G. W.; Schlegel, H. B.; Scuseria, G. E.; Robb, M. A.; Cheeseman, J. R.; Scalmani, G.; Barone, V.; Mennucci, B.; Petersson, G. A.; Nakatsuji, H.; Caricato, M.; Li, X.; Hratchian, H. P.; Izmaylov, A. F.; Bloino, J.; Zheng, G.; Sonnenberg, J. L.; Hada, M.; Ehara, M.; Toyota, K.; Fukuda, R.; Hasegawa, J.; Ishida, M.; Nakajima, T.; Honda, Y.; Kitao, O.; Nakai, H.; Vreven, T.; Montgomery, J. J. A.; Peralta, J. E.; Ogliaro, F.; Bearpark, M.; Heyd, J. J.; Brothers, E.; Kudin, K. N.; Staroverov, V. N.; Kobayashi, R.; Normand, J.; Raghavachari, K.; Rendell, A.; Burant, J. C.; Iyengar, S. S.; Tomasi, J.; Cossi, M.; Rega, N.; Millam, J. M.; Klene, M.; Knox, J. E.; Cross, J. B.; Bakken, V.; Adamo, C.; Jaramillo, J.; Gomperts, R.; Stratmann, R. E.; Yazyev, O.; Austin, A. J.; Cammi, R.; Pomelli, C.; Ochterski, J. W.; Martin, R. L.; Morokuma, K.; Zakrzewski, V. G.; Voth, G. A.; Salvador, P.; Dannenberg, J. J.; Dapprich, S.; Daniels, A. D.; Farkas, O. Foresman, J. B.; Ortiz, J. V.; Cioslowski, J.; Fox, D. J. *Gaussian Development Version*; Gaussian Inc.: Wallingford, CT, 2010.
(40) The parameters were downloaded from dftb.org (accessed Dec 06, 2010).
(41) Jancu, J.-M.; Scholz, R.; Beltram, F.; Bassani, F. *Phys. Rev. B* **1998**, *57*, 6493–6507.
(42) Heringer, D.; Niehaus, T. A.; Wanko, M.; Frauenheim, T. *J. Comput. Chem.* **2007**, *28*, 2589.
(43) Hratchian, H. P.; Parandekar, P. V.; Raghavachari, K.; Frisch, M. J.; Vreven, T. *J. Chem. Phys.* **2008**, *128*, 034107.
(44) Frauenheim, T.; Weich, F.; Kohler, T.; Uhlmann, S.; Porezag, D.; Seifert, G. *Phys. Rev. B* **1995**, *52*, 11492.
(45) Festa, G.; Cossi, M.; Barone, V.; Cantele, G.; Ninno, D.; Iadonisi, G. *J. Chem. Phys.* **2005**, *122*, 184714.
(46) Cantele, G.; Trani, F.; Ninno, D.; Cossi, M.; Barone, V. *J. Phys.: Condens. Matter* **2006**, *18*, 2349–2365.
(47) Barone, V.; Cimino, P. *Chem. Phys. Lett.* **2008**, *454*, 139–143.
(48) Elstner, M. *J. Phys. Chem. A* **2007**, *111*, 5614–5621.
(49) Otte, N.; Scholten, M.; Thiel, W. *J. Phys. Chem. A* **2007**, *111*, 5751–5755.
(50) Pan, W.; Zhu, T.; Yang, W. *J. Chem. Phys.* **1997**, *107*, 3981–3985.
(51) Santos, H.; Ujaque, G.; Ramos, M.; Gomes, J. *J. Comput. Chem.* **2006**, *27*, 1892–1897.
(52) Barone, V.; Cacelli, I.; Ferretti, A.; Monti, S.; Prampolini, G. *Phys. Chem. Chem. Phys.* **2009**, *11*, 10644–10656.
(53) Barone, V.; Cacelli, I.; Ferretti, A.; Monti, S.; Prampolini, G. *Phys. Chem. Chem. Phys.* **2010**, *12*, 4201–9.